



## Fabrication of pervaporative composite PDMS.MWCNT/PES membrane for ethanol/water separation

Amirhossein Farahi, Ghasem D. Najafpour\*, Aliasghar Ghoreyshi

Biotechnology Research Laboratory, Faculty of Chemical Engineering, Noushirvani University of Technology, Babol, Iran, emails: najafpour@nit.ac.ir (G.D. Najafpour), Amirhossein\_farahi@yahoo.com (A. Farahi), Aa\_ghoreyshi@nit.ac.ir (A. Ghoreyshi)

Received 11 April 2018; Accepted 28 September 2018

### ABSTRACT

A dense, thin, and hydrophobic active layer of polydimethylsiloxane (PDMS) on polyethersulfone (PES) along with desired additives such as polyvinylpyrrolidone (PVP), polyethylene glycol (PEG), and SiO<sub>2</sub> as support layers was successfully fabricated. The effect of types of support layers on ethanol separation in pervaporation process was investigated. With desired composite PDMS/PES. PVP (having 76% porosity), ethanol separation factor and total flux were 6.25 and 440 g/m<sup>2</sup>.h, respectively. In order to enhance membrane's ethanol selectivity, specific additives were added; in fact, extra improvements in ethanol separation with novel membrane were performed. To improve the hydrophobicity of the fabricated membrane, multiwalled carbon nanotubes (MWCNT's) with several weight percentages were added to the active layer of the composite membrane matrix. At desired percentage of MWCNT (3 wt.%) and total flux of 420 g/m<sup>2</sup>.h, the ethanol separation factor was enhanced by 26.4%.

*Keywords:* Bioethanol; Pervaporation; Polydimethylsiloxane composite membrane; Multiwalled carbon nanotubes

### 1. Introduction

Bioethanol as green fuel is an efficient octane booster; also has special feature to be considered as an alternative fuel. Due to high energy demand and fossil fuel depletion, an alternative renewable source of energy is required to supply fuel demand. High emission of fossil fuel, carbon mono and dioxides may cause greenhouse gases and global warming. Use of green fuel may result in less gas emission and carbon dioxide generated from renewable sources should easily be entered into atmosphere for photosynthetic process. Bioethanol as a desired fuel obtained via fermentation of carbohydrates derived from biomass can be produced from renewable carbon sources such as corn, sorghum, cellulose, and algal biomass via fermentation process [1–9].

In fermentation of ethanol, the mixture of ethanol/water should be separated; the process is energy intensive. Although, distillation process is often used for the separation

of ethanol, but this process is required high energy and utility costs [5]. In fact, bioethanol should not be invasive without any improvement in reducing energy requirements [10]. In order to solve this problem, among different types of separation methods, pervaporation (PV), is an attractive in ethanol separation [3,11]. In PV process, it is possible for us to produce highly concentrated ethanol using ethanol selective membranes [5]. PV technology, compared with traditional separation technology such as distillation, molecular sieve, and extraction, has many advantages: high separation efficiency, low energy consumption and simple operation, and low utility costs [12,13]. Partial vaporization of a liquid through a dense polymeric membrane is called PV [14,15]. PV is one of the membrane technologies that utilize a dense and nonporous membranes for separation [16]. The process is commonly operated under vacuum in downstream side of the membrane; because of an evaporative phase change usually occurred [7,17]. Gao et al. [18] implemented PDMS/PS membrane to separate water and alcohol (8 wt.%) in PV process. They have found ethanol separation factor and total flux

\* Corresponding author.

of 6.4 and 265 g/m<sup>2</sup>.h, respectively. Esfahanian et al. [2,9] used polydimethylsiloxane (PDMS) membrane in PV process. They have successfully separated ethanol/water with ethanol productivities of 1.41 and 6.49 g/L.h in batch and continuous bioreactor ethanol fermentations, respectively.

Among the composite membranes for ethanol/water separation in PV process, the PDMS is one of the most interesting membranes that have been extensively studied as selective layer in PV process [3]. PDMS has a high selectivity toward ethanol because of its amorphous molecular structure and rubbery state at ambient temperature [19,20]. The support layers in composite membranes were mainly polysulfones, polyimides, polyetherimides, polyethersulfones (PESs), polyimides, polyvinylidene fluoride, cellulose acetate, and polyesters [16,20–29]. Often, fillers such as polyvinylpyrrolidone were added to the support layers for different purposes such as improvement of surface roughness and total flux enhancement. Shahrabi et al. [27] used PES membranes with various additives including polyvinylpyrrolidone (PVP) and polyethylene glycol (PEG) as support layers on the composite PDMS membranes. The effect of support layers on water/toluene separation process was investigated. The results indicated that use of support layer with higher porosity increased the process flux by maintaining the value of separation factor. Lauren et al. [30] investigated on performance of PES membrane with various additives. Among the membranes, addition of PVP into the PES membrane enhanced the flux in separation process.

A mixed matrix membranes (MMMs) consist of a base polymer with additive fillers. Several kinds of fillers such as nanosilica, zeolite, nanoiron, and carbon black (CB) were used to increase ethanol selectivity. These unique fillers were individually added into PDMS polymer casting solutions [31,32]. Extensive studies have been performed on the effect of carbon-based fillers such as CB, graphene, and carbon nanotubes (CNT) into the matrix of polymeric membrane for the improvement of the selectivity in gas separation process [33–37]. Sanip et al. [36] made MMMs and investigated the effect of addition of CNTs on CO<sub>2</sub>/CH<sub>4</sub> gas separation process. It was observed that the addition of 0.5–10 wt.% of CNT has improved the membrane separation factor by 100% in gas separation. Nour et al. [34] investigated on the effect of addition of CNTs in PDMS membranes on H<sub>2</sub>/CH<sub>4</sub> gas separation. The results indicated that addition of 1 wt.% of multiwalled carbon nanotubes (MWCNT) to PDMS membrane has enhanced the separation factor by 94.8%.

In this study, different PDMS composite membranes for ethanol/water separation were fabricated. In order to evaluate the ethanol separation factor at different conditions, the fabricated composite membranes were tested in PV process. For fabrication of composite membranes, PES membrane as support layer was synthesized by phase inversion method. Effects of addition of some filler such as PVP, PEG, and SiO<sub>2</sub> in PES support layer on composite membrane performance were investigated. The prepared support membranes were studied by means of porosity and contact angle. The membrane surface morphology and structure were characterized using atomic force microscopy (AFM) and field emission scanning electron microscopy (FESEM). Then, PDMS as an ethanol selective and dense layer was established on the support layer. Ethanol selectivity and flux of the fabricated

composite membranes in a PV process were examined. In the following stage, the effects of MWCNT as filler on PDMS membrane matrix were studied. All necessary analyzes for characterization such as AFM and FESEM were fully conducted. Finally, the performances of the fabricated membranes were compared with literature and commercial composite membranes.

## 2. Experimental

### 2.1. Materials

PES Ultrason E6020 with molecular weight of 58,000 Da was supplied (BASF, Germany). Dimethylacetamide (DMAc), dibutyltindilaurate, tetraethyl orthosilicate (TEOS), and *n*-heptane were purchased (Merck, Germany). Analytical grade PDMS having viscosity of 150 cSt., PVP K90 with molecular weight of 360,000 Da and PEG with molecular weight of 400 Da were supplied (Aldrich, USA). Glycerol was purchased (Scharlau, Spain). MWCNT 99% pure carbon was obtained from PPKK, Universiti Sains Malaysia [38]; the characteristic and physical properties of MWCNT are summarized in Table 1.

A commercial composite membrane by effective thickness of 5 μm PDMS top layer was supplied by Pervatech Company (the Netherland). A support consisting of PET with thickness of 100 μm as the sublayer to assure the mechanical strength of the membrane and an intermediate UF membrane polyimide (PI) as the first membrane layer with thickness of 150 μm were used in PV process.

### 2.2. Membrane support

Asymmetric layers of PES with additives such as polyvinylpyrrolidone, PEG, and SiO<sub>2</sub> were prepared for support layers via phase inversion technique. This technique is explained by the following method: homogeneous solutions including PES, additives (PVP, PEG, and SiO<sub>2</sub>), and DMAc as solvents were defined based on weight percentages [27,39]. Based on literature survey on combination and blend of mixture of PEG, PVP, and SiO<sub>2</sub>; the weight percentages of PVP, PEG, and SiO<sub>2</sub> as additives were 2 wt.% [27,39]. Table 2 summarized the chemical composition of membrane supports. The coagulation temperature was reported to be 40°C.

The prepared blends of solutions were casted on a glass plate at room temperature. An automatic casting machine was designed with constant speed to spread out uniformly

Table 1  
Characteristic and physical properties of MWCNT

Property	Value	Method of measurement
Average diameter, nm	6.2 ± 0.5	TEM
Average length, μm	1–5	TEM
Carbon purity, %	>99	TGA
Residuals, %	<1	TGA
Amorphous carbon, %	<0.1	TGA
Degree of graphitization, $I_D/I_G$ ratio	0.575	Raman

Table 2  
Chemical composition of membrane support

Type of membrane support	PES (wt.%)	DMAc (wt.%)	Additives (wt.%)	Ref.
PES	16	84	0	[27,39]
PES and PVP	16	82	2	[27,39]
PES and PEG	16	82	2	[27,39]
PES and SiO <sub>2</sub>	16	82	2	[27,39]

the polymeric solution with high accuracy in thickness and repeatability of the fabricated membrane. The thicknesses of all the support layers were set 100  $\mu\text{m}$ . The glass plate was immediately immersed in the coagulation bath. The formed layer was stored in distilled water for 48 h. At the final stage, the film was washed out with distilled water and then dried and kept at room temperature for 48 h.

### 2.3. Preparation of composite membrane with active layer

For preparation of the active layer on support layer, PDMS with different weight composition ratio was dissolved in *n*-heptane solution. The weight ratios of PDMS, cross-linking agent (TEOS) and dibutyltin dilaurate as catalyst were 10:1:0.2 in the solution. The solution was stirred for 2 h at room temperature. In order to reduce mass transfer resistance due to penetration of PDMS solution into the porous substrate of porous support layer, prior to coating, the PES support is prewetted by glycerol and the excess glycerol was wiped off by filter paper [27]. The support layer was pasted on a glass plate and the PDMS solution was uniformly casted on its surface. The active layers were allowed to be partially cross-linked at room temperature for duration of 24 h. The composite membrane was heat-treated put in an oven set at 70°C for 4 h to complete the cross-linkage.

### 2.4. Nanocomposite membranes preparation using CNT in PDMS

For the fabrication of polymeric nanocomposites membranes, four different MWCNT/PDMS nanocomposite membranes with MWCNT weight percentages of 1, 3, 5, and 10 wt.% were prepared [34]. MWCNT's were dispersed in toluene, to facilitate effective, and uniform dispersion of MWCNT within the PDMS viscous matrix. The toluene/MWCNT suspension was then added to PDMS by vigorous mixing. This suspension (PDMS polymer, toluene solvent, and MWCNT weight percentages of 1, 3, 5, and 10wt.%) was sonicated in an ultrasonic bath (XB2 Ultrasonic Bath,

England) for 0.5 h. In the next step, the suspension was mechanically stirred for 1 h at 70°C to evaporate the toluene solvent. The suspension was allowed to cool down to room temperature, then PDMS solvent (*n*-heptane) was added to the mixture. The cross-linking agent and the catalyst were dissolved in the solution based on Table 3. The mixture was stirred for 2 h before casting and then the solution was casted on the support layer. The active layers were cross-linked at room temperature for 24 h and then it was heat treated in an oven set at 70°C for 4 h to complete the cross-linking phenomena.

### 2.5. Characterization

The membrane surfaces were characterized using AFM. The AFM analyses were performed under AFM microscope (Nanosurf easy scan2 flex, Switzerland). On different areas of each membrane sample, the values of surface roughness were determined. At least three different locations were examined and the average values of surface roughness were reported. The roughness was expressed as root mean square and surface roughness (RMS and  $R_a$ ) values. The  $R_a$  and RMS were defined as the average area of roughness and the root mean square roughness of the surface, respectively.

The cross-sectional morphologies of the fabricated membranes were characterized by FESEM using a Hitachi FESEM model S-4160 (Hitachi, Japan,). For the cross-sectional images, the membranes were fractured after immersion in liquid nitrogen. All samples were stocked on a conductive sample holder with double-sided copper tape. The membrane samples were coated under vacuum by a thin layer of gold with a sputtering system.

To measure the hydrophobicity of the membranes, contact angle was performed. The contact angle of membranes was measured by kruss-contact angle measuring system-G10 (Germany). A water drop (5  $\mu\text{L}$ ) was lowered onto the membrane's surface from a needle tip. A magnified image of the droplet was recorded by a digital camera. Static contact angles were determined from these images with automated software. The contact angle measurement was taken as the mean value of 5 different points on each membrane sample. If the angle is less than 90°, the surface of the membrane is hydrophilic, and if it is more than 90°, the membrane is hydrophobic.

To determine the support membrane porosity, the dry membranes were cut in a definite size and then immersed in distilled water for 1 d. Water on the surface of the membrane was removed with a filter paper and the sample membrane was weighed ( $W_w$ ). Then the membrane sample was dried for 24 h in a desiccator and weighed again to determine the

Table 3  
Chemical composition of solute in nano composite PDMS.MWCNT casting solution

Type of composite membrane	PDMS (wt.%)	MWCNT (wt.%)	Cross-linker (wt.%)	Catalyst (wt.%)
PDMS.MWCNT (1 wt.%)	30	1	3	0.6
PDMS.MWCNT (3 wt.%)	30	3	3	0.6
PDMS.MWCNT (5 wt.%)	30	5	3	0.6
PDMS.MWCNT (10 wt.%)	30	10	3	0.6

membrane sample dry weight ( $W_d$ ). The membrane porosity ( $\epsilon$ ) was calculated by the following equation:

$$\epsilon = \frac{W_w - W_d}{\rho V} \quad (1)$$

where  $\rho$  is density of water at the room temperature and  $V$  is the volume of the membrane in wet state.

The composite membrane swelling degree (SD) is defined as a piece of membrane is weighted and immersed in the solution at room temperature for 24 h. The surface of sample is then wiped by filter paper and then weighed. The SD is calculated by the following expression:

$$SD = \frac{W_2 - W_1}{W_1} \quad (2)$$

where  $W_1$  (g) and  $W_2$  (g) are the weights of samples before and after immersion, respectively.

### 2.6. Pervaporation

In PV, the membrane was installed in the PV cell. The feed stream of ethanol by concentrations of 2–20 wt.% was prepared. Vacuum on the permeate side was maintained by vacuum pump (Edwards, England). Vapor-side pressure was kept at lower than 2 mmHg. Permeate vapor was trapped in a liquid nitrogen trap at  $-196^\circ\text{C}$ . Two cold traps using liquid nitrogen were set in parallel allowing the collection of permeate. Then the sample was weighed and analyzed by high-performance liquid chromatography (Smartline, Knauer, Germany). HPLC column was Eurokat H (Knauer, Germany). The oven temperature was set at  $75^\circ\text{C}$ . The sample size, eluent, and flow rate were 20  $\mu\text{L}$ ,  $\text{H}_2\text{SO}_4$  (0.01 N), and 0.5 mL/min, respectively.

The calculation for permeation of flux ( $J$ ) was defined as follows:

$$J = \frac{m}{(\Delta t \times A)} \quad (3)$$

Also, membrane selectivity toward gas mixtures and mixtures of organic liquids is usually expressed in terms of separation factor ( $\alpha$ ) defined as follows:

$$\alpha = \frac{(y_{\text{alcohol}} / y_{\text{water}})}{(x_{\text{alcohol}} / x_{\text{water}})} \quad (4)$$

where  $m$  is the total amount of permeate collected during the experimental period,  $\Delta t$  of 1 h at steady state;  $A$  is the effective membrane area,  $x$  and  $y$  represent the mole fractions of a component in the feed and permeate, respectively [40].

## 3. Results and discussion

Special composite ethanol selective membranes, PES membrane supports with a dense layer of PDMS were fabricated and characterized. The developed membranes were used in pervaporative ethanol separation process.

### 3.1. Membrane support

Several mixtures of PES, PVP, PEG, and  $\text{SiO}_2$  were used for casting membrane supports. Fig. 1 shows FESEM of the cross-sectional images of PES membrane supports along with PEG 2 wt.%, PVP 2 wt.%, and  $\text{SiO}_2$  2 wt.%.

The membrane support without any additive (Fig. 1(a)) has a finger-like structure. Once PEG added to PES, there were no significant changes observed in the membrane morphology and the same finger-like structure can be seen in Fig. 1(b). Addition of PVP to PES created wide channel-like macrovoids with open end channels (Fig. 1(c)).  $\text{SiO}_2$  addition resulted in finger-like structure with some thin channel-like structure with close end (Fig. 1(d)). The surface images of four types of membrane supports were investigated by AFM. Based on AFM results, addition of fillers and additives to PES support layer has created high surface roughness. The surface roughness ( $R_a$ ) of PES without additive was about 7.2 nm. The average roughness by addition of PEG, PVP, and  $\text{SiO}_2$  to PES increased to 12, 24, and 10.48 nm, respectively.

The contact angle between membrane and water was directly measured using an optical contact angle instrument. The porosities of membrane supports were determined using Eq. (1). Characterization of membrane supports is summarized in Table 4.

Generally, additive with high molecular weight in compare with low molecular weight have increased the porosity of support layer. That is probably due to increase in replacement speed of organic solvent and water at phase inversion stage. Therefore, PES support with PVP (molecular weight of 360 kDa) has the highest porosity. Also, based on obtained data, PES.PVP has the highest surface roughness among the investigated support membranes. Increasing surface roughness decreases the contact angle; that has subsequently resulted in increase in membrane total flux.

### 3.2. Effect of fabricated support layers on pervaporation

PDMS mixture as active layer was casted on four kinds of fabricated support layers and the performances of these composite membranes were investigated in PV process for separation of ethanol in dilute ethanol/water mixture. Fig. 2 depicts total flux and ethanol separation factor of composite membranes with respect to types of support layers. Based on obtained results, as the roughness of support layers increased the composite membrane flux also increased; while the ethanol separation factor slightly decreased.

In next stages of experiments, based on obtained data for maximum flux (440  $\text{g}/\text{m}^2\cdot\text{h}$ ) and reasonable ethanol separation factor (6.25), the mixture of PES and PVP was selected as support layer for the preparation of composite membrane applied in PV process.

### 3.3. Composite membrane

Fig. 3 illustrates the FESEM cross-sectional images of the fabricated composite membranes. The PDMS mixture as hydrophobic active layer was casted for the thickness of  $20 \mu\text{m} \pm 5$  on the support layers (PES, PES.PEG, PES.PVP, and PES. $\text{SiO}_2$ ) which had thickness of  $100 \mu\text{m} \pm 5$ .

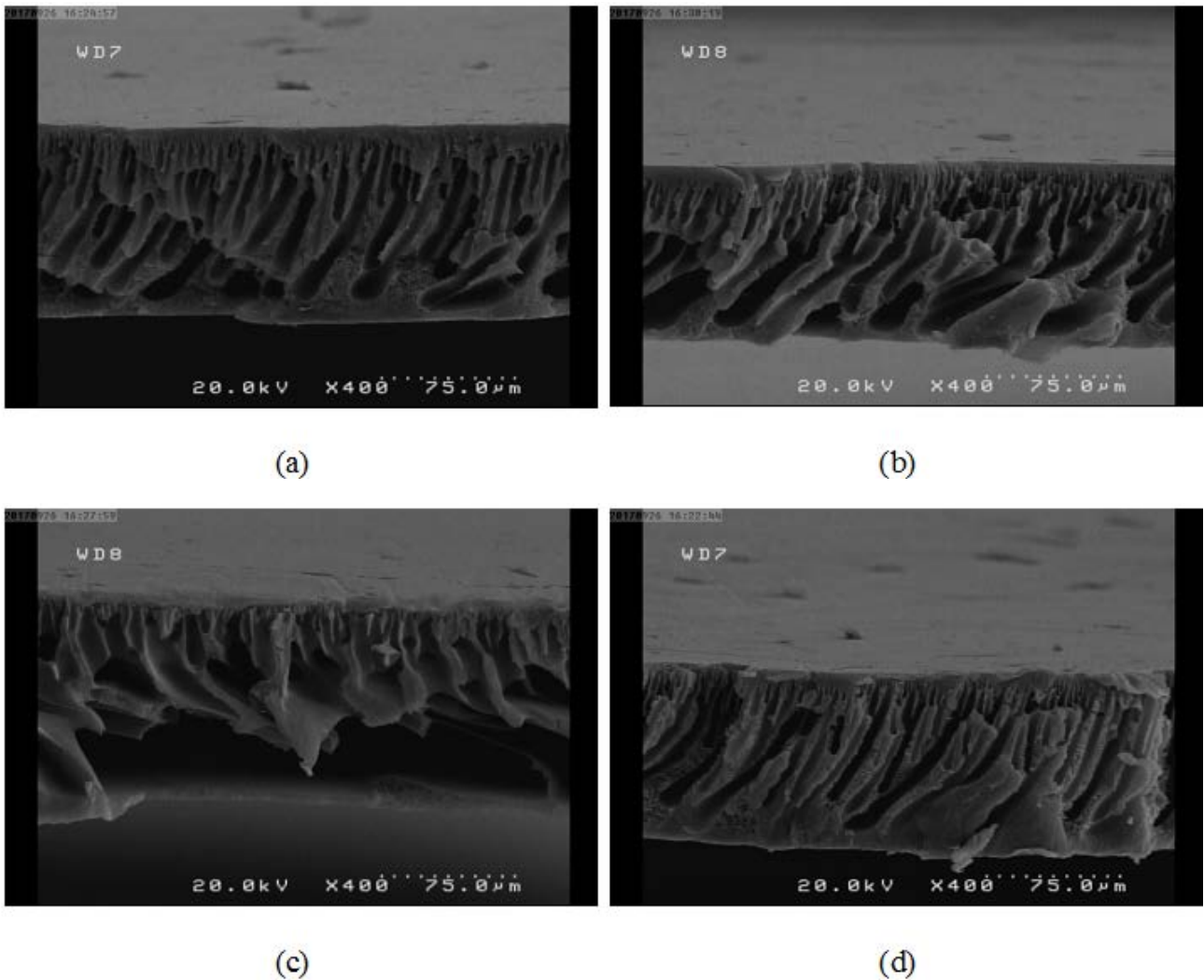


Fig. 1. FESEM images of PES membrane support; (a) PES 16 wt.%, (b) PES 16 wt.% and PEG 2 wt.%, (c) PES 16 wt.% and PVP 2 wt.%, (d) PES 16 wt.% and SiO<sub>2</sub> 2 wt.%.

Table 4  
Characterization of membrane supports

Membranes	Contact angle (°)	Porosity (%)	Surface roughness (nm)
PES	81	51	7.2
PES and PEG	78	64	12
PES and PVP	71	76.5	24
PES and SiO <sub>2</sub>	79.5	54	10.48

As explained in Section 3.2, the PES.PVP was selected as the best support layer for preparation of the composite membrane applied in PV process. For more clarification about the fabricated membrane, the cross-sectional FESEM images at two different magnifications, top surface FESEM image, and AFM surface image of PDMS/PES.PVP are shown in Fig. 4. In Figs. 4(a) and (b), two magnifications of cross-sectional FESEM images of composite PDMS/PES.PVP membrane were placed. Fig. 4(c) shows the top surface of FESEM

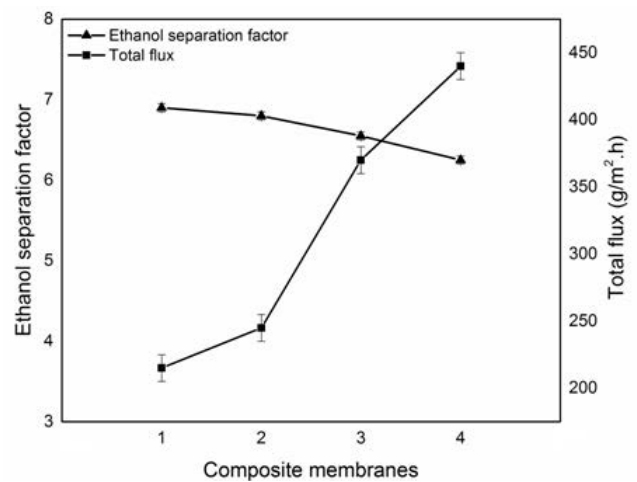


Fig. 2. Effect of fabricated support layers on pervaporation; (1) PDMS/PES, (2) PDMS/PES.SiO<sub>2</sub>, (3) PDMS/PES.PEG, (4) PDMS/PES.PVP, PDMS 30 wt.%, Temp. 25°C, and feed ethanol 2 wt.%.

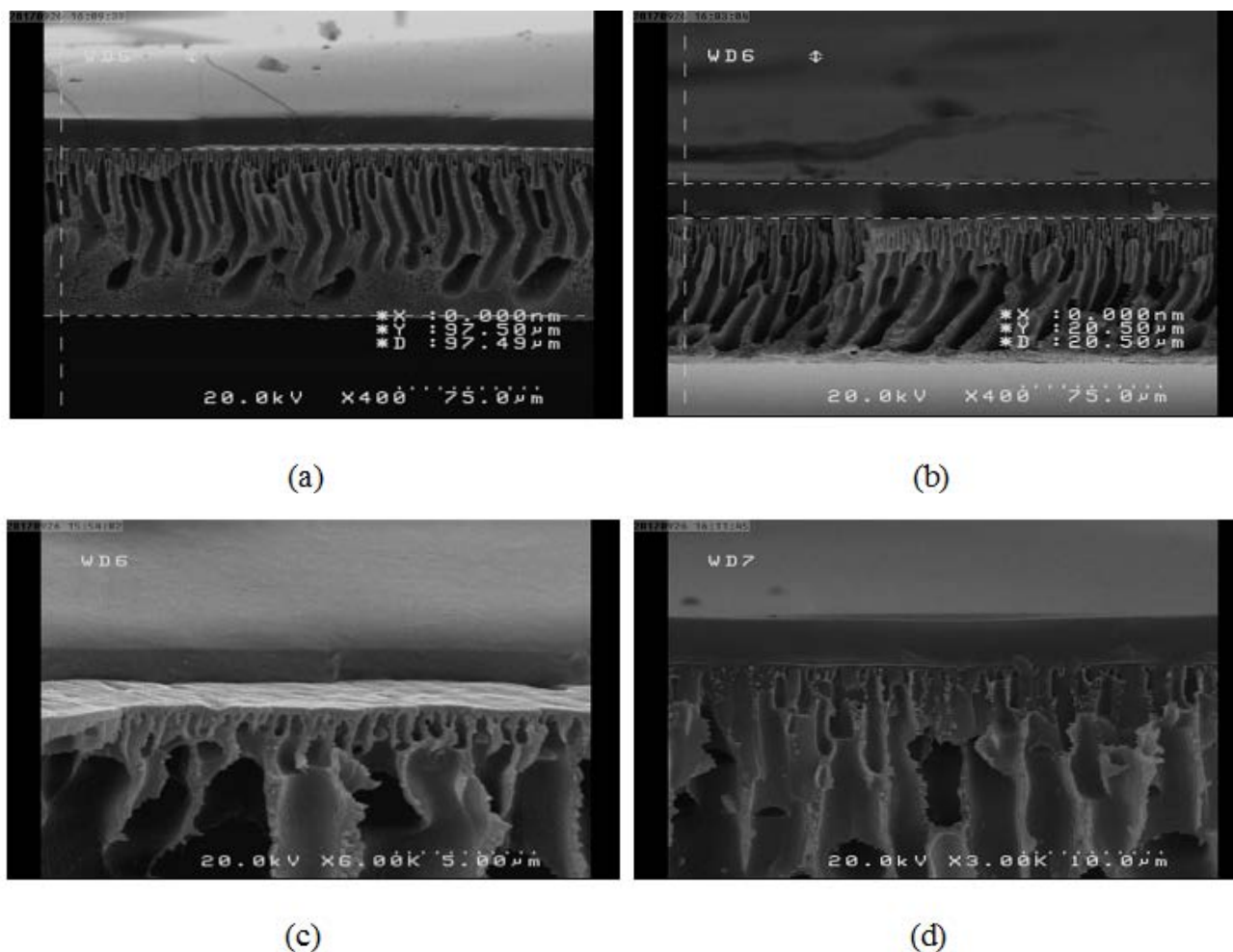


Fig. 3. FESEM cross-sectional images of fabricated composite membrane; (a) PDMS/PES, (b) PDMS/PES.PEG, (c) PDMS/PES.PVP, and (d) PDMS/PES.SiO<sub>2</sub>.

image of the composite PDMS/PES.PVP membrane. Fig. 4(d) depicts the AFM surface image of composite PDMS/PES.PVP membrane. The PDMS mixture as hydrophobic active layer was casted for the thickness of  $20 \mu\text{m} \pm 5$  on PES.PVP support layers, which had thickness of  $100 \mu\text{m} \pm 5$ . As is illustrated the active layer is a dense layer on porous support membrane for application in PV process. The surface roughness ( $R_a$ ) of the composite PDMS/PES.PVP membranes was 0.621 nm. Comparison between support membrane roughness and composite membranes roughness proved that active layer is formed on the support layer. In fact, in preparation of composite membrane dense layer is placed on top of the rough surface of membrane support. Finally, deposition of selective layer resulted in low surface roughness.

#### 3.4. Effect of PDMS concentration on pervaporation

In the next step, the concentration of PDMS as selective layer on PES.PVP support layer was varied from 10 to 50 wt.%. An automated machine was designed and fabricated for membrane casting; the thickness was fixed while concentration of PDMS was varied. All PDMS solutions were casted on PES.PVP support layer by constant thickness of

$20 \mu\text{m} \pm 5$ . As the concentration of dense layer of PDMS on membrane support increased the flux has decreased while the ethanol separation factor increased (Fig. 5). That was due to high affinity of the top layer to ethanol at high PDMS concentration.

Selection of the most desired condition is based on suitable PDMS concentration for desired flux and desired value for ethanol separation factor. In fact, both flux and selectivity were important in PV process. Therefore, the selective layer of PDMS having 30 wt.% was selected for the next stage of experiments.

#### 3.5. Effect of ethanol concentration in feed on pervaporation

The effect of ethanol concentrations (2–20 wt.%) on PV at constant temperature (25°C) with the defined concentration of composite PDMS (30 wt.)/PES.PVP (2 wt.%) was experimented. The effect of ethanol concentration on the membrane flux and ethanol selectivity is illustrated in Fig. 6.

As ethanol concentration increased in feed stream the total flux improved. In fact, high ethanol concentration caused membrane swelling; as a result, separation factor decreased. Based on obtained results, the SD and the

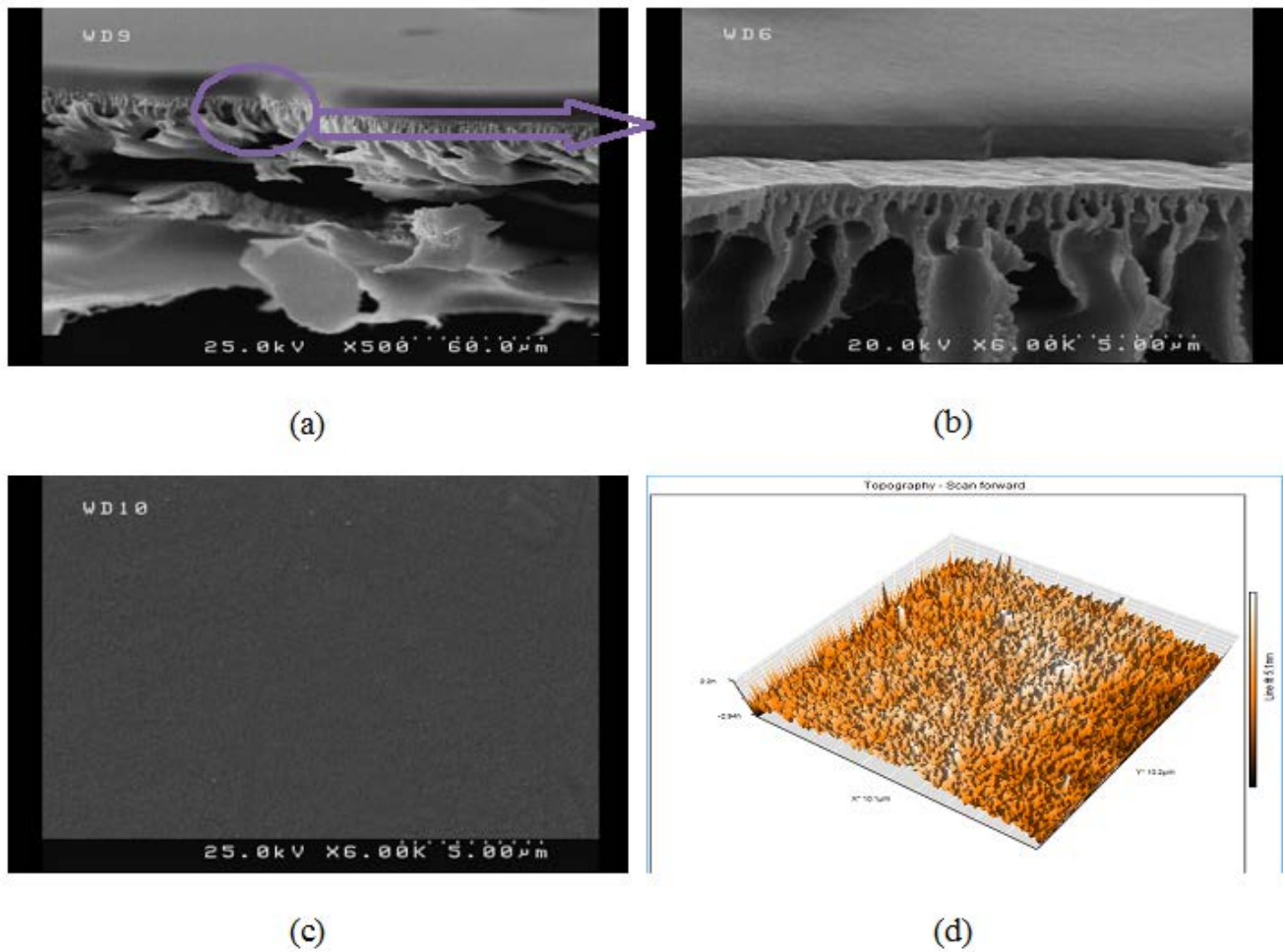


Fig. 4. (a) and (b) Cross-sectional FESEM images of composite PDMS/PES.PVP membrane by two magnification, (c) Top surface FESEM image of composite PDMS/PES.PVP membrane, (d) AFM surface image of composite PDMS/PES.PVP membrane.

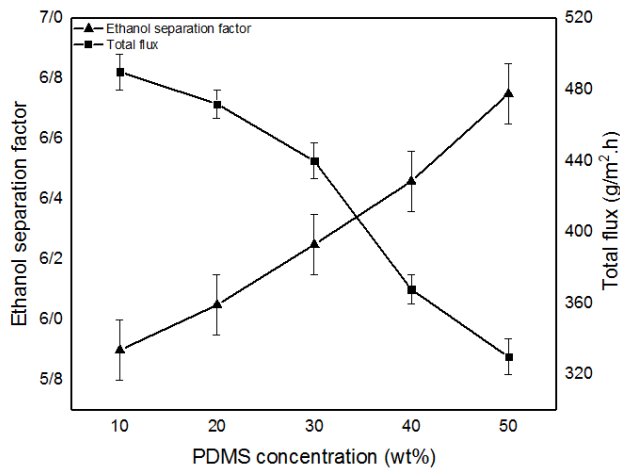


Fig. 5. Effect of PDMS concentration on total flux and ethanol separation factor, temp. 25°C, feed ethanol 2 wt%.

polymer cross-linkage density have inverse relationship. As a result, increase in the SD, PDMS polymer cross-linkage density has decreased and more water was penetrated into the membrane. Therefore, permeation total flux has increased and ethanol separation factor has decreased. The SD was monitored while ethanol concentration in the feed stream increased (Fig. 7). When ethanol concentration increased from 2 to 20 wt.%, the SD has increased by 4%; as a result, 14.4% ethanol separation factor decreased.

### 3.6. Effect of feed temperature on pervaporation

The effect of feed temperature (25°C, 35°C, and 45°C) on PV at constant ethanol concentration in feed (2 wt.%) with composite PDMS (30 wt.)/PES.PVP (2 wt.%) membrane was experimented. The obtained results for the effect of feed temperature on the membrane flux and ethanol selectivity is shown in Fig. 8.

As illustrated in Fig. 8, increasing temperature increases permeation flux and decreases ethanol separation factor. These changes occurred due to the fact that during PV, molecules diffused through free volumes of the polymeric selective membrane. Thermal motions of polymer chains

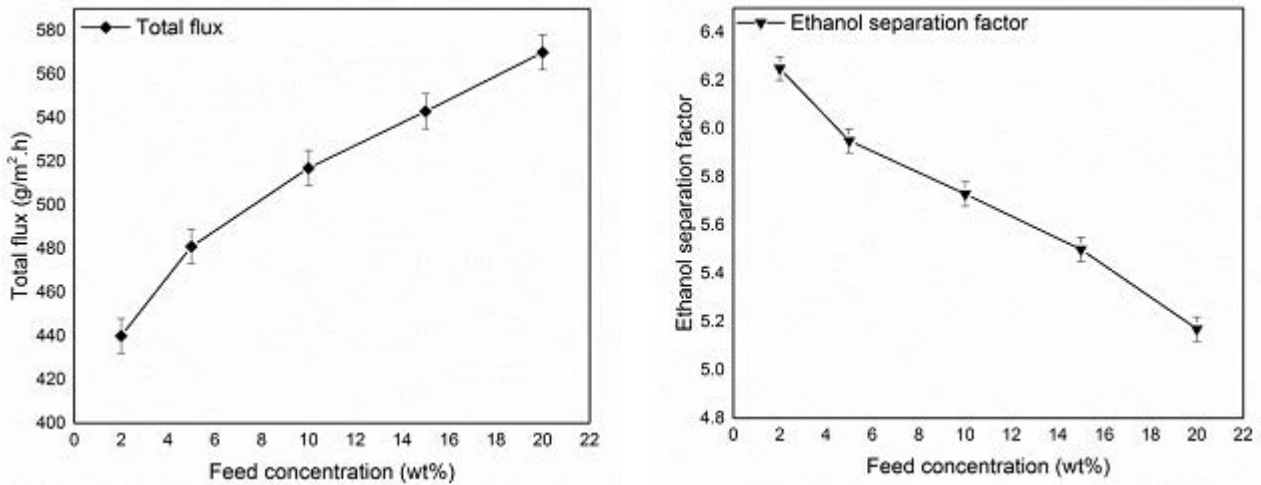


Fig. 6. Effect of feed concentration on; (a) total flux, (b) separation factor, temp. 25°C, PDMS concentration 30 wt.%.

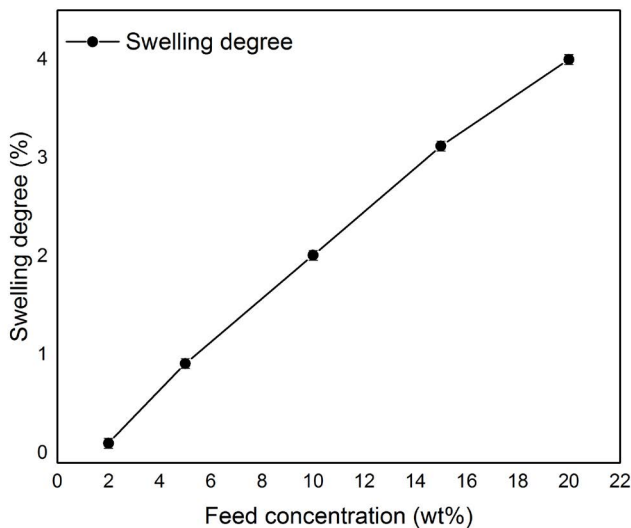


Fig. 7. Swelling degree in different feed concentrations.

produced free volumes in amorphous regions. As temperature increases, frequency and amplitude of polymer jumping chains increase [15]. As a result, free volume of the PDMS polymeric membrane increases and more water molecules can penetrate into the membrane. Therefore, permeation of total flux has increased and ethanol separation factor has slightly decreased.

### 3.7. Effect of MWCNT in composite PDMS/PES membrane

The FESEM cross-sectional images of MWCNT in composite membrane are shown in Fig. 9.

Composite MWCNT.PDMS/PES membranes are shown in Fig. 9(a). At high magnification of the image, multiwalled carbon nanotubes in the composite membrane are easily observed in Fig. 9(b). The MWCNT's were blended in active layer matrix. The top surface layer FESEM images of composite MWCNT.PDMS membranes with MWCNT weight percentages of 1, 3, 5, and 10wt.% are shown in Fig. 10.

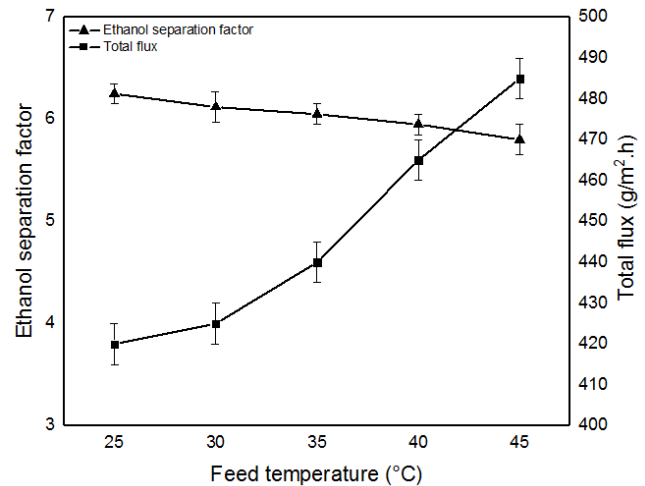


Fig. 8. Effect of feed temperature on ethanol separation factor and total flux, PDMS concentration (30 wt.%), feed ethanol (2 wt.%).

The images in Figs. 10(a) and (b) show MWCNT dispersion was reasonably homogenous in the active layer; in contrary Figs. 10(c) and (d) depict a massive coagulation formed due to high concentration of MWCNT in PDMS active layer.

Fig. 11 shows AFM surface image of the composite membrane by addition of MWCNT into active layer. In fact, addition of MWCNT in the composite membrane has created high surface roughness. Addition of MWCNT from 1 to 10 wt.% resulted in average roughness ( $R_a$ ) of 4.4–26 nm, respectively.

Fig. 12(a) depicts ethanol separation factor with respect to MWCNT concentration in the PDMS composite membrane for ethanol/water separation. As the concentration of MWCNT in PDMS selective layer increased, the ethanol separation factor in PV process has substantially increased. As illustrated in Fig. 11, the roughness has increased by the enrichment of MWCNT concentration. In hydrophobic surface, by increasing the surface roughness the contact angle has

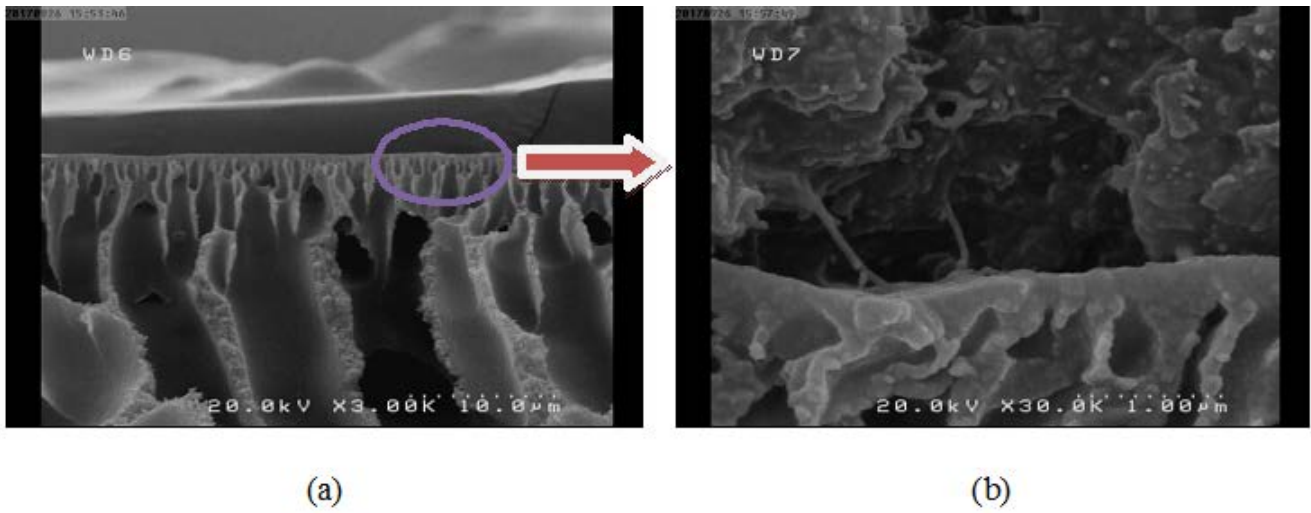


Fig. 9. Cross-sectional FESEM images of composite PDMS.MWCNT (3 wt.%) /PES.PVP membrane; (a) magnification 3,000, (b) magnification 30,000.

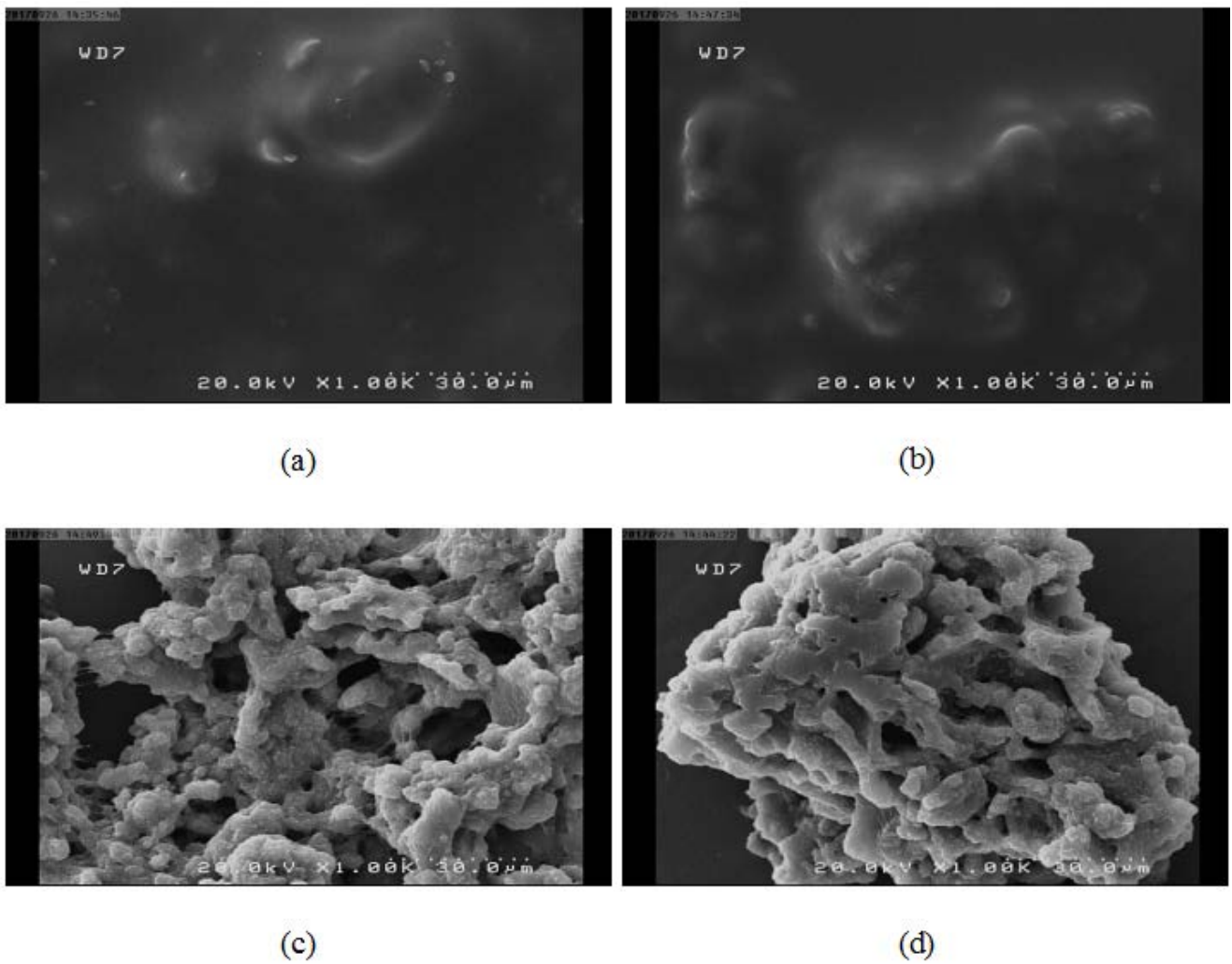


Fig. 10. FESEM images of top surface MWCNT.PDMS nanocomposite membranes with MWCNT; (a) 1 wt.%, (b) 3 wt.%, (c) 5 wt.%, and (d) 10 wt.%.

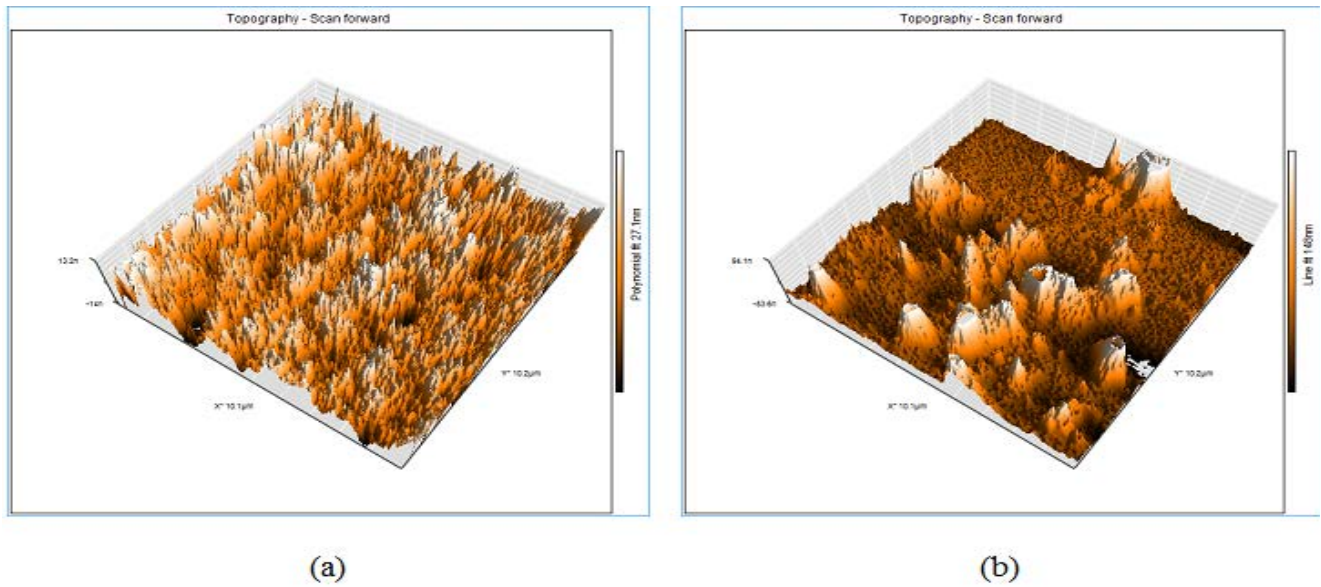


Fig. 11. AFM images in nanocomposite membrane for; (a) MWCNT (1 wt.%) and (b) MWCNT (10 wt.%).

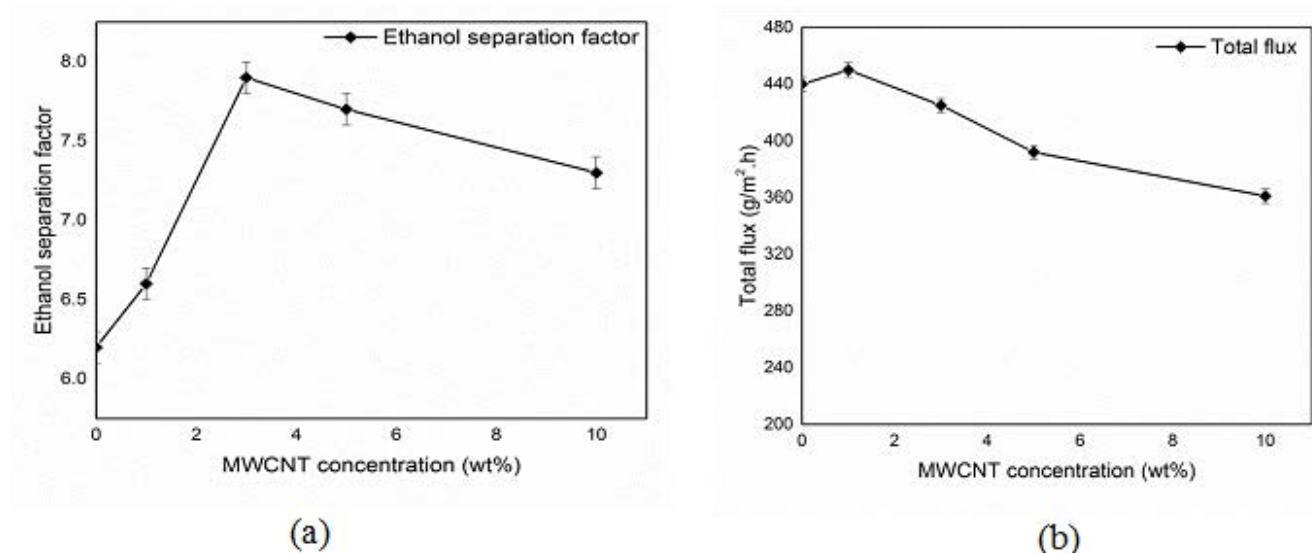


Fig. 12. Effect of MWCNT concentration on; (a) ethanol separation factor, (b) ethanol flux.

to increase; that is, due to improvement of hydrophobicity of the membrane [41]. Therefore, by improvement of the hydrophobicity, the ethanol separation factor has increased. But when the concentration of the MWCNT increased more than 3 wt.% the separation factor gradually decreased. At high MWCNT concentration (>3 wt.%) the coagulation similar to cluster was formed. Based on obtained data the most desired value for MWCNT concentration is defined 3 wt.%, which has resulted in separation factor of 7.9. In fact, addition of MWCNT up to 3 wt.% was in favor of ethanol separation factor while behind that concentration caused decrease in membrane performance.

Fig. 12(b) illustrates when the MWCNT is added to the composite membrane, initially the total flux slightly increased that is due to MWCNT act as filler; then, the flux

decreased which is due to high hydrophobicity of membrane. By increasing in hydrophobicity less water can penetrate into nanocomposite membrane. As a result, the permeation total flux has decreased. Therefore, when the MWCNT concentration increased beyond certain point, by enhancement of hydrophobicity of the membrane flux has decreased.

### 3.8. Fabricated composite membrane versus data in literature and commercial membrane

Based on experimental results for ethanol 2 wt.% as feed, the ethanol separation factor for commercial composite membrane was 6.5 and total flux of 375 g/m<sup>2</sup>.h was obtained. Comparison between commercial composite membrane data and experimental results obtained in this work for

Table 5  
Comparison between several types of membrane for ethanol separation

Membrane type	Separation factor	Flux (g/m <sup>2</sup> /h)	Feed ethanol concentration (wt.%)	Ref.
Fabricated PDMS/PES.PVP	6.25	440	2	Present work
Novel fabricated PDMS.MWCNT/PES.PVP	7.9	420	2	Present work
Commercial PDMS/PET/PI	6.5	375	2	Present work
PDMS-PS graft copolymer	6.2	130	10	[42]
PDMS-PI graft copolymer	6.6	320	6.6	[43]
PDMS-PS IPN supported membrane	5.5	160	2	[44]
PDMS/PEI/PPP	3.7	270	5	[25]
PDMS/PS	6.4	265	8	[18]
POMS	5	380	2	[45]
PDMS/PEI(hollow-fiber)	7–9	231–252	1–10	[46]
PDMS/PA	6	850	2	[16]
PDMS/CA	2.5	650	2	[16]

the fabricated membrane showed improvement in ethanol separation factor using MWCNT. Due to high ethanol separation factor in blended PDMS. MWCNT (3 wt.)/PES.PVP (2 wt.%) composite membrane was determined 7.9 and total flux of 420 g/m<sup>2</sup>.h was obtained. In this study, the fabricated composite MWCNT.PDMS/PES.PVP membrane improved the commercial composite membrane for ethanol separation by 21.5% with more total flux in PV process. The performance of fabricated composite PDMS (30 wt.%) MWCNT (3 wt.)/PES.PVP (2 wt.%) was compared with reported data in literature. Table 5 summarizes a comparison study for several types of PDMS composite membrane for ethanol separation factor and flux. Based on obtained data in this work the performance of fabricated membrane is justified as a suitable with high ethanol separation performance for PV process.

#### 4. Conclusion

In the study, the polymeric composite PDMS/PES membrane was fabricated for ethanol separation in PV process. Addition of suitable additives to PES support membrane enhanced porosity and surface roughness of the support layer; that resulted in membrane total flux to increase while the ethanol separation factor has slightly decreased.

Increase in ethanol separation factor and decrease in total flux were observed by increasing PDMS concentration in active layer of composite membrane. By increasing the ethanol concentration in the feed stream, the ethanol factor decreased due to increase in SD of the polymeric membrane matrix.

Addition of MWCNT to PDMS selective layer resulted in significant increase in ethanol separation factor; while hydrophobicity of the composite membrane increased. MWCNT addition more than 3 wt.% caused coagulation and cluster formation in the PDMS selective layer that caused to decrease in separation factor.

#### Acknowledgments

Authors gratefully acknowledge Biotechnology Research Laboratory, Noshirvani University of Technology for the

facilities provided to conduct the present research. Also, special thanks are extended to Nezhadgholi and Alizadeh Foundation (Babol, Iran) for the financial support of present research through research grant.

#### References

- [1] A. El-Sebaei, S. Shalaby, Solar drying of agricultural products: a review, *Renew. Sustain. Energy Rev.*, 16 (2012) 37–43.
- [2] M. Esfahanian, A.S. Rad, S. Khoshhal, G. Najafpour, B. Asghari, Mathematical modeling of continuous ethanol fermentation in a membrane bioreactor by pervaporation compared to conventional system: genetic algorithm, *Bioresour. Technol.*, 212 (2016) 62–71.
- [3] C. Fu, D. Cai, S. Hu, Q. Miao, Y. Wang, P. Qin, Z. Wang, T. Tan, Ethanol fermentation integrated with PDMS composite membrane: an effective process, *Bioresour. Technol.*, 200 (2016) 648–657.
- [4] F.J. Gómez-Gil, X. Wang, A. Barnett, Energy production of photovoltaic systems: fixed, tracking, and concentrating, *Renew. Sustain. Energy Rev.*, 16 (2012) 306–313.
- [5] T. Ikegami, H. Yanagishita, D. Kitamoto, H. Negishi, K. Haraya, T. Sano, Concentration of fermented ethanol by pervaporation using silicalite membranes coated with silicone rubber, *Desalination*, 149 (2002) 49–54.
- [6] P.S. Nigam, A. Singh, Production of liquid biofuels from renewable resources, *Prog. Energy Combust. Sci.*, 37 (2011) 52–68.
- [7] P. Peng, B. Shi, Y. Lan, A review of membrane materials for ethanol recovery by pervaporation, *Sep. Sci. Technol.*, 46 (2010) 234–246.
- [8] U.K. Rout, A. Voß, A. Singh, U. Fahl, M. Blesl, B.P.Ó. Gallachóir, Energy and emissions forecast of China over a long-time horizon, *Energy*, 36 (2011) 1–11.
- [9] M. Esfahanian, A. Ghorbanfarahi, A. Ghoreyshi, G. Najafpour, H. Younesi, A. Ahmad, Enhanced bioethanol production in batch fermentation by pervaporation using a PDMS membrane bioreactor, *Int. J. Eng. Trans. B*, 25 (2012) 249.
- [10] P.D. Chapman, T. Oliveira, A.G. Livingston, K. Li, Membranes for the dehydration of solvents by pervaporation, *J. Membr. Sci.*, 318 (2008) 5–37.
- [11] S. Fan, Z. Xiao, Y. Zhang, X. Tang, C. Chen, W. Li, Q. Deng, P. Yao, Enhanced ethanol fermentation in a pervaporation membrane bioreactor with the convenient permeate vapor recovery, *Bioresour. Technol.*, 155 (2014) 229–234.
- [12] J. Chen, J. Li, R. Qi, H. Ye, C. Chen, Pervaporation performance of crosslinked polydimethylsiloxane membranes for deep desulfurization of FCC gasoline: I. Effect of different sulfur species, *J. Membr. Sci.*, 322 (2008) 113–121.

- [13] J. Li, C. Chen, B. Han, Y. Peng, J. Zou, W. Jiang, Laboratory and pilot-scale study on dehydration of benzene by pervaporation, *J. Membr. Sci.*, 203 (2002) 127–136.
- [14] E. Favre, Temperature polarization in pervaporation, *Desalination*, 154 (2003) 129–138.
- [15] T. Mohammadi, A. Aroujalian, A. Bakhshi, Pervaporation of dilute alcoholic mixtures using PDMS membrane, *Chem. Eng. Sci.*, 60 (2005) 1875–1880.
- [16] M. Rezakazemi, K. Shahidi, T. Mohammadi, Synthetic PDMS composite membranes for pervaporation dehydration of ethanol, *Desal. Wat. Treat.*, 54 (2015) 1542–1549.
- [17] D. O'Brien, J. Craig, Ethanol production in a continuous fermentation/membrane pervaporation system, *Appl. Microbiol. Biotechnol.*, 44 (1996) 699–704.
- [18] J. Guo, G. Zhang, W. Wu, S. Ji, Z. Qin, Z. Liu, Dynamically formed inner skin hollow fiber polydimethylsiloxane/poly-sulfone composite membrane for alcohol permselective pervaporation, *Chem. Eng. J.*, 158 (2010) 558–565.
- [19] Y.K. Hong, W.H. Hong, Influence of ceramic support on pervaporation characteristics of IPA/water mixtures using PDMS/ceramic composite membrane, *J. Membr. Sci.*, 159 (1999) 29–39.
- [20] D. Sun, B.-B. Li, Z.-L. Xu, Pervaporation of ethanol/water mixture by organophilic nano-silica filled PDMS composite membranes, *Desalination*, 322 (2013) 159–166.
- [21] Y. Chen, T. Miyano, A. Fouda, T. Matsuura, Preparation and gas permeation properties of silicone-coated dry polyethersulfone membranes, *J. Membr. Sci.*, 48 (1990) 203–219.
- [22] M. Hyder, R. Huang, P. Chen, Effect of selective layer thickness on pervaporation of composite poly (vinyl alcohol)-poly (sulfone) membranes, *J. Membr. Sci.*, 318 (2008) 387–396.
- [23] M.-D. Jia, K.-V. Pleinemann, R.-D. Behling, Preparation and characterization of thin-film zeolite-PDMS composite membranes, *J. Membr. Sci.*, 73 (1992) 119–128.
- [24] L. Li, Z. Xiao, S. Tan, L. Pu, Z. Zhang, Composite PDMS membrane with high flux for the separation of organics from water by pervaporation, *J. Membr. Sci.*, 243 (2004) 177–187.
- [25] M. Osorio-Galindo, A. Iborra-Clar, I. Alcaina-Miranda, A. Ribes-Greus, Characterization of poly (dimethylsiloxane)-poly (methyl hydrogen siloxane) composite membranes for organic water pervaporation separation, *J. Appl. Polym. Sci.*, 81 (2001) 546–556.
- [26] C. Page, A. Fouda, T. Matsuura, Pervaporation performance of polyetherimide membranes spin-and dip-coated with polydimethylsiloxane, *J. Appl. Polym. Sci.*, 54 (1994) 975–989.
- [27] S.S. Shahrabi, H. Mortaheb, J. Barzin, M. Ehsani, Pervaporative performance of a PDMS/blended PES composite membrane for removal of toluene from water, *Desalination*, 287 (2012) 281–289.
- [28] F.J. Tsai, D. Kang, M. Anand, Thin-film-composite gas separation membranes: on the dynamics of thin film formation mechanism on porous substrates, *Sep. Sci. Technol.*, 30 (1995) 1639–1652.
- [29] X. Zhan, J.-D. Li, J. Chen, J.-Q. Huang, Pervaporation of ethanol/water mixtures with high flux by zeolite-filled PDMS/PVDF composite membranes, *Chin. J. Polym. Sci.*, 27 (2009) 771–780.
- [30] L.F. Greenlee, N.S. Rentz, Influence of nanoparticle processing and additives on PES casting solution viscosity and cast membrane characteristics, *Polymer*, 103 (2016) 498–508.
- [31] B.M. Novak, Hybrid nanocomposite materials between inorganic glasses and organic polymers, *Adv. Mater.*, 5 (1993) 422–433.
- [32] L. Romasanta, M. Lopez-Manchado, R. Verdejo, The role of carbon nanotubes in both physical and chemical liquid–solid transition of polydimethylsiloxane, *Eur. Polym. J.*, 49 (2013) 1373–1380.
- [33] S. Kim, T.W. Pechar, E. Marand, Poly (imide siloxane) and carbon nanotube mixed matrix membranes for gas separation, *Desalination*, 192 (2006) 330–339.
- [34] M. Nour, K. Berean, S. Balendhran, J.Z. Ou, J. Du Plessis, S. McSweeney, M. Bhaskaran, S. Sriram, K. Kalantar-zadeh, CNT/PDMS composite membranes for H<sub>2</sub> and CH<sub>4</sub> gas separation, *Int. J. Hydrogen Energy*, 38 (2013) 10494–10501.
- [35] M. Nour, K. Berean, M.J. Griffin, G.I. Matthews, M. Bhaskaran, S. Sriram, K. Kalantar-Zadeh, Nanocomposite carbon-PDMS membranes for gas separation, *Sens. Actuators*, 161 (2012) 982–988.
- [36] S. Sanip, A.F. Ismail, P. Goh, T. Soga, M. Tanemura, H. Yasuhiko, Gas separation properties of functionalized carbon nanotubes mixed matrix membranes, *Sep. Purif. Technol.*, 78 (2011) 208–213.
- [37] A.D. Kiadehi, M. Jahanshahi, A. Rahimpour, S.A.A. Ghoreyshi, The effect of functionalized carbon nano-fiber (CNF) on gas separation performance of polysulfone (PSf) membranes, *Chem. Eng. Process.*, 90 (2015) 41–48.
- [38] K.F. Yee, Y.T. Ong, A.R. Mohamed, S.H. Tan, Novel MWCNT-buckypaper/polyvinyl alcohol asymmetric membrane for dehydration of etherification reaction mixture: fabrication, characterisation and application, *J. Membr. Sci.*, 453 (2014) 546–555.
- [39] Z.L. Xu, F.A. Qusay, Effect of polyethylene glycol molecular weights and concentrations on polyethersulfone hollow fiber ultrafiltration membranes, *J. Appl. Polym. Sci.*, 91 (2004) 3398–3407.
- [40] M. Molder, Basic principles of membrane technology, Kluwer Academic Publishers, 1996.
- [41] T.C. Hobæk, K.G. Leinan, H.P. Leinaas, C. Thaulow, Surface nanoengineering inspired by evolution, *BioNano Sci.*, 1 (2011) 63.
- [42] S. Takegami, H. Yamada, S. Tsujii, Pervaporation of ethanol/water mixtures using novel hydrophobic membranes containing polydimethylsiloxane, *J. Membr. Sci.*, 75 (1992) 93–105.
- [43] T. Kashiwagi, K. Okabe, K. Okita, Separation of ethanol from ethanol/water mixtures by plasma-polymerized membranes from silicone compounds, *J. Membr. Sci.*, 36 (1988) 353–362.
- [44] L. Liang, E. Ruckenstein, Pervaporation of ethanol-water mixtures through polydimethylsiloxane-polystyrene interpenetrating polymer network supported membranes, *J. Membr. Sci.*, 114 (1996) 227–234.
- [45] A. Aroujalian, A. Raisi, Pervaporation as a means of recovering ethanol from lignocellulosic bioconversions, *Desalination*, 247 (2009) 509–517.
- [46] H.J. Lee, E.J. Cho, Y.G. Kim, I.S. Choi, H.J. Bae, Pervaporative separation of bioethanol using a polydimethylsiloxane/polyetherimide composite hollow-fiber membrane, *Bioresour. Technol.*, 109 (2012) 110–115.